

Monte Carlo calculations of correction factors for plane-parallel ionization chambers in clinical electron dosimetry

Fujio Araki^{a)}

Department of Radiological Technology, Kumamoto University School of Health Sciences,
4-24-1, Kuhonji, Kumamoto, 862-0976, Japan

(Received 30 March 2008; revised 10 July 2008; accepted for publication 16 July 2008;
published 13 August 2008)

Recent standard dosimetry protocols recommend that plane-parallel ionization chambers be used in the measurements of depth-dose distributions or the calibration of low-energy electron beams with beam quality $R_{50} < 4 \text{ g/cm}^2$. In electron dosimetry protocols with the plane-parallel chambers, the wall correction factor, P_{wall} , in water is assumed to be unity and the replacement correction factor, P_{repl} , is taken to be unity for well-guarded plane-parallel chambers, at all measurement depths. This study calculated P_{wall} and P_{repl} for NACP-02, Markus, and Roos plane-parallel chambers in clinical electron dosimetry using the EGSnrc Monte Carlo code system. The P_{wall} values for the plane-parallel chambers increased rapidly as a function of depth in water, especially at lower energy. The value around R_{50} for NACP-02 was about 10% greater than unity at 4 MeV. The effect was smaller for higher electron energies. Similarly, P_{repl} values with depth increased drastically at the region with the steep dose gradient for lower energy. For Markus P_{repl} departed more than 10% from unity close to R_{50} due to the narrow guard ring width. P_{repl} for NACP-02 and Roos was close to unity in the plateau region of depth-dose curves that includes a reference depth, d_{ref} . It was also found that the ratio of the dose to water and the dose to the sensitive volume in the air cavity for the plane-parallel chambers, $D_w/[D_{\text{air}}]_{\text{pp}}$, at d_{ref} differs significantly from that assumed by electron dosimetry protocols. © 2008 American Association of Physicists in Medicine.
[DOI: 10.1118/1.2968102]

Key words: wall correction factor, replacement correction factor, plane-parallel ionization chamber, electron dosimetry, Monte Carlo calculations

I. INTRODUCTION

Recent standard dosimetry protocols¹⁻⁴ recommend that plane-parallel ionization chambers be used in depth-dose measurements for high-energy electron beams. This is because the replacement correction factor P_{repl} for cylindrical ionization chambers is not known well as a function of a depth in water. In electron dosimetry protocols with the plane-parallel chambers, the wall correction factor P_{wall} , in water is assumed to be unity and P_{repl} is taken to be unity for well-guarded plane-parallel chambers, at all measurement depths. Plane-parallel chambers are also recommended for the calibration of low-energy electron beams with beam qualities $R_{50} < 4 \text{ g/cm}^2$ or less than $\bar{E}_0 = 10 \text{ MeV}$, because the depth of measurement is more unambiguously defined. R_{50} is defined as the half-value depth of a dose in water.

Monte Carlo calculations are a good method of investigating P_{wall} and P_{repl} factors. Sempau *et al.*⁵ evaluated beam quality factors for plane-parallel chambers using the PENELOPE system. Their results show that the overall perturbation factor (the product of P_{wall} and P_{repl}) at the reference depth d_{ref} for the NACP-02 and PPC-40 chambers is different by approximately 0.5% at low electron energy ($R_{50} = 1.4 \text{ cm}$) compared to that of the TRS-398 protocol when the factor is assumed to be unity at $R_{50} = 8.75 \text{ cm}$. Recently, Buckley and Rogers⁶ calculated the P_{wall} correction for the combination of a water phantom and wall materials of plane-parallel cham-

bers (NACP-02, Markus and Roos, etc.), using the EGSnrc Monte Carlo user-code CSnrc. When compared to the assumptions of standard dosimetry protocols, which use P_{wall} values of unity in electron beams, the calculated P_{wall} values show corrections of 1.7%–0.8% at d_{ref} , for an NACP-02 chamber, over a range of nominal energies from 5 MeV ($R_{50} = 2.08 \text{ cm}$) to 21 MeV ($R_{50} = 8.3 \text{ cm}$). Similarly, the P_{wall} values are 1.25%–0.4% and 1.2%–0.5% for Roos and Markus chambers, respectively. The P_{wall} values are also more than 6% greater than unity with increasing depth of measurement at 6 MeV. Verhaegen *et al.*⁷ also reported P_{wall} values as a function of depth of measurement for the NACP-02 chamber in a water phantom. More recently, Zink and Wulff⁸ calculated P_{wall} values at d_{ref} in water for the Roos chamber. The investigations of Verhaegen *et al.*⁷ and Zink and Wulff⁸ are calculated using the same EGSnrc Monte Carlo system with different user-codes and show similar results to those of Buckley and Rogers.⁶ McEwen *et al.*⁹ used an empirical method for the determination of P_{wall} for the NACP-02 chamber. The effect is up to 1.4% at $R_{50} = 1.2 \text{ cm}$ and shows a slightly smaller perturbation than Monte Carlo calculations. The results mentioned above indicate that the size of the P_{wall} correction for plane-parallel chambers should be estimated adequately in the electron dosimetry protocol.

In contrast, work on the P_{repl} correction^{6,8,10} for plane-parallel chambers using Monte Carlo calculations is limited

to the values for the NACP-02 and Roos chambers at d_{ref} in water, and only for an NACP-02 chamber as a function of depth of measurement in water. Recent work by Buckley and Rogers⁶ and Verhaegen *et al.*⁷ indicated the need for a replacement correction at depths greater than d_{ref} . More recently, Wang and Rogers¹⁰ investigated the P_{repl} correction for the NACP-02 chamber as a function of depth of measurement in water in more detail. The correction depends on depth of measurement and varies from 0.992 to 1.035 at a depth between 0.5 cm and R_{50} for a 6 MeV ($R_{50}=2.63$ cm) beam. P_{repl} for NACP-02 is 0.9964 even at d_{ref} and the value is different from unity assumed in the electron dosimetry protocol.

The purpose of this study was to investigate the P_{wall} and P_{repl} correction factors for NACP-02, Markus and Roos chambers at a depth between near-surface and R_{50} . The Markus chamber with a very small guard ring is a classic design and thus not recommended in recent codes of practice. However, the bench marking of the perturbation effects for the Markus chamber is a valuable contribution for previous experimental data. Both correction factors were calculated by the EGSnrc Monte Carlo code system in a range of 4 MeV ($R_{50}=1.31$ cm) to 18 MeV ($R_{50}=7.6$ cm) electron beams. Also, the ratio of the dose to water and the dose to the sensitive volume in the air cavity for the plane-parallel chambers was compared with the water-to-air stopping-power ratio to evaluate the overall correction factor. Furthermore, the dose ratio at d_{ref} was compared with that assumed by the TG-51 and TRS-398 protocols.

II. THEORY

The relationship of the dose to water, D_w , and the dose to air in water, D_{air} , is presented according to the Spencer–Attix cavity theory

$$D_w = D_{\text{air}} \left(\frac{\bar{L}}{\rho} \right)_{\text{air}}^w. \quad (1)$$

$(\bar{L}/\rho)_{\text{air}}^w$ is the average restricted mass collision stopping-power ratio of water to air. This formulation is based on an idealized case in which the wall and the air cavity of the ionization chamber do not perturb the electron spectrum.

In actual measurement, the presence of the chamber wall and the cavity will affect the electron fluence spectrum and therefore corrections are required to the Spencer–Attix cavity theory. The absorbed dose to water for a plane-parallel chamber can be expressed using two corrections as follows:

$$D_w = [D_{\text{air}}]_{\text{pp}} \left(\frac{\bar{L}}{\rho} \right)_{\text{air}}^w P_{\text{wall}} P_{\text{repl}}. \quad (2)$$

$[D_{\text{air}}]_{\text{pp}}$ is the dose to the sensitive volume in the air cavity for the chamber. P_{wall} accounts for the nonphantom equivalence of the chamber wall material. P_{repl} is the product of two components, P_{fl} and P_{gr} . P_{fl} is the fluence correction factor that corrects for changes in the electron fluence spectrum due to the presence of the air cavity, predominantly the in-scattering of electrons that makes the electron fluence in-

TABLE I. Characteristics of clinical electron beams from the Varian Clinac linear accelerators. The reference depth d_{ref} is obtained from $0.6R_{50}-0.1$ (cm).

Machine	E_{nominal} (MeV)	R_{50} (cm)	d_{ref} (cm)
2100C	4	1.31	0.69
21EX	6	2.37	1.32
	9	3.59	2.05
	12	5.06	2.94
	15	6.27	3.66
	18	7.60	4.46

side the cavity different from that in the medium in the absence of the cavity. For many plane-parallel chambers, P_{fl} is assumed to be unity, but is taken to be nonunity for chambers which are not well guarded. P_{gr} is the gradient correction factor that accounts for the shift upstream of the effective point of measurement of the chamber due to the cavity. For plane-parallel chambers, P_{gr} is taken as unity when the point of measurement is at the front of the air cavity.

III. METHODS AND MATERIALS

III.A. Monte Carlo simulations

The EGSnrc (Ref. 11)/BEAMnrc code (Refs. 12 and 13) was used to simulate electron beams emerging from a Varian Clinac linear accelerator (Varian Oncology Systems, Palo Alto, CA). The modeling of Monte Carlo simulations for an electron beam is described in previous papers.^{14,15} Phase space data were taken below the applicator with a 15×15 cm² field size for all electron energies. The dose distributions for electron beams in water were calculated with the EGSnrc/DOSXYZnrc code¹⁶ using the phase space data as input. The SSD was 100 cm. The parameters used for simulation were: AE=0.521 MeV, ECUT=0.700 MeV, and AP=PCUT=0.01 MeV. The CPU used was a Pentium IV with a 3.2 GHz processor. The incident electron energy was adjusted to agree within 2% between Monte Carlo calculated and measured dose distributions (central axis depth-dose curve and off-axis dose profile at a depth of dose maximum) in a water phantom. Table I presents the characteristics of

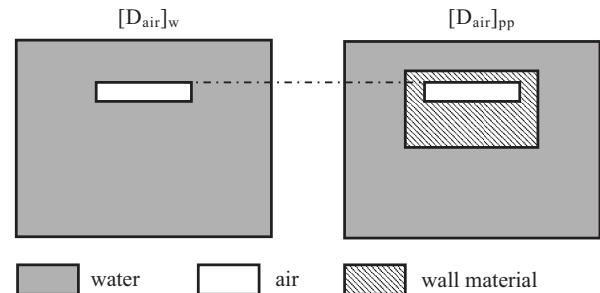


FIG. 1. Simplified schematic diagram of the two geometries used to compute P_{wall} . P_{wall} is computed as the ratio of doses $[D_{\text{air}}]_w/[D_{\text{air}}]_{\text{pp}}$ using the CAVRZnrc code. $[D_{\text{air}}]_w$ is the dose to the sensitive volume in the air cavity for a chamber wall composed entirely of water, and $[D_{\text{air}}]_{\text{pp}}$ is the dose to a chamber with a detailed model of the realistic chamber wall.

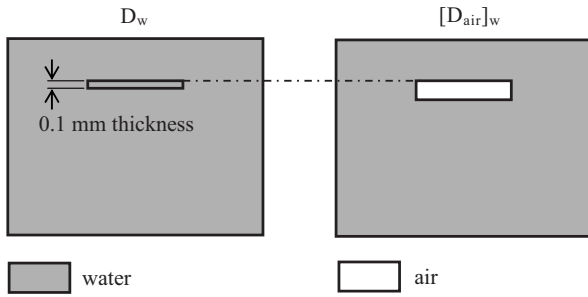


FIG. 2. Schematic diagram of the two geometries used to compute P_{repl} . P_{repl} is computed from the relationship of the ratio of doses $D_w/[D_{\text{air}}]_w$ and the water-to-air stopping-power ratio shown in Eq. (3) in text. D_w is the dose to water and calculated for a 0.1 mm thick slab with a front face at a depth in water equal to the point of measurement for the chamber. The ratio of doses and the stopping-power ratio are calculated using the DOSRZnrc, CAVRZnrc, and SPRRZnrc codes.

clinical electron beams from the Varian Clinac linear accelerators used in this study.

Phase space data scored were also used to calculate wall correction factors and replacement correction factors for plane-parallel chambers, and Spencer–Attix water-to-air stopping-power ratios. Both correction factors and stopping-power ratios were calculated using EGSnrc user-codes CAVRZnrc,¹⁷ DOSRZnrc,¹⁷ and SPRRZnrc.¹⁷ The doses calculated in the cavity and the phantom affect energy thresholds for photon and electron transport, AE and ECUT. Wang and Rogers¹⁰ demonstrated that the cavity and phantom doses calculated with AE=0.512 MeV are about 0.5% lower than with AE=0.521 MeV at a depth of R_{50} in a 6 MeV

electron beam, but the phantom/cavity dose ratio is not dependent (at the 0.1% level) on the ECUT and AE values from 1 to 20 keV. Also, the water-to-air stopping-power ratios are not very sensitive to the ECUT value and vary less than 0.3% for ECUT ranging from 5 to 20 keV, at depths between 0.5 and 3 cm in the 6 MeV beam.¹⁰ Thus, the energy thresholds for user-codes were set to AE=ECUT=0.521 MeV and AP=PCUT=0.01 MeV in this study.

III.B. Calculation of wall correction factor P_{wall} and replacement correction factor P_{repl}

The values of P_{wall} and P_{repl} for plane-parallel chambers were calculated at a depth between near-surface and R_{50} using Monte Carlo methods. Figure 1 shows a schematic representation of how the calculation geometries are arranged to compute the P_{wall} correction factor. P_{wall} was computed as the ratio of doses $[D_{\text{air}}]_w/[D_{\text{air}}]_{\text{pp}}$ using the CAVRZnrc code. $[D_{\text{air}}]_w$ is the dose to the sensitive volume in the air cavity for a chamber wall composed entirely of water. The volume is defined by the electrode diameter and the separation. $[D_{\text{air}}]_{\text{pp}}$ is the dose to a real chamber geometry shown in Eq. (2). Figure 1 demonstrates simple chamber geometries, but in CAVRZnrc calculations, detailed chamber geometries were used according to the manufacturers' specifications.

The P_{repl} correction factor was computed from the relationship of the ratio of doses $D_w/[D_{\text{air}}]_w$ in the calculation geometries shown in Fig. 2 and the water-to-air stopping-power ratios. D_w is the dose to water and calculated for a 0.1 mm thick slab with a front face at a depth in water equal to the point of measurement, using the DOS-

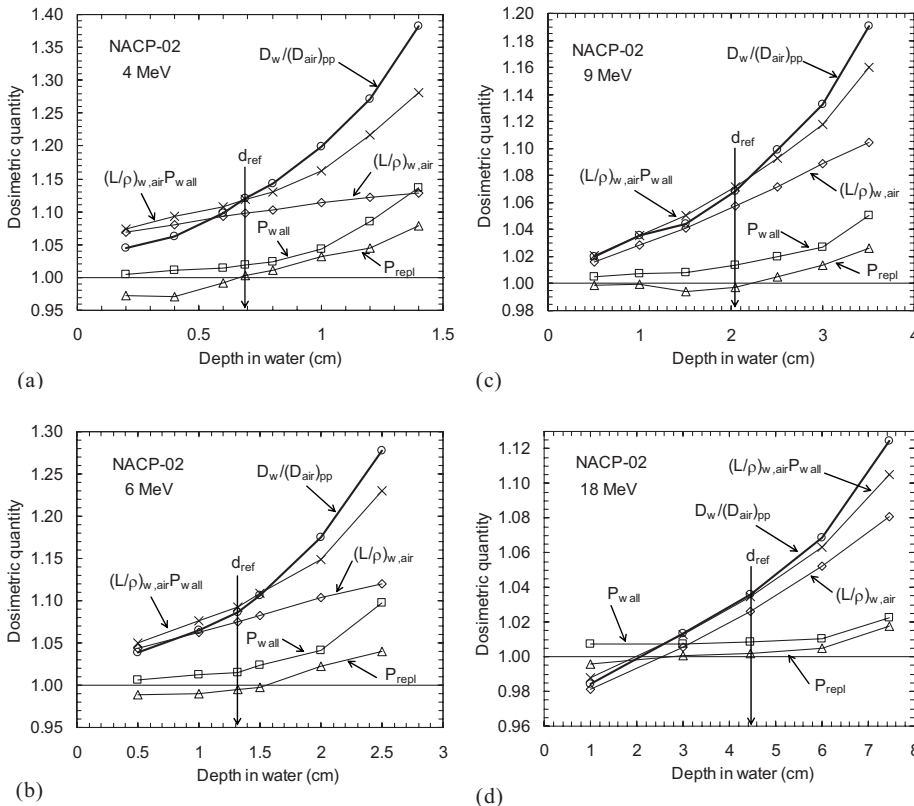


FIG. 3. Calculated dosimetric quantities for an NACP-02 chamber as a function of depth at (a) 4, (b) 6, (c) 9, and (d) 18 MeV beams. For the NACP-02 chamber, the protocol assumes that the ratio of doses $D_w/[D_{\text{air}}]_{\text{pp}}$ is equal to the water-to-air stopping-power ratio, but the dose ratio directly depends on the variation of P_{wall} and P_{repl} values. The dose ratio at a reference depth d_{ref} agrees with the product $(\bar{L}/\rho)_{\text{air}}^w P_{\text{wall}}$ because the P_{repl} value is close to unity.

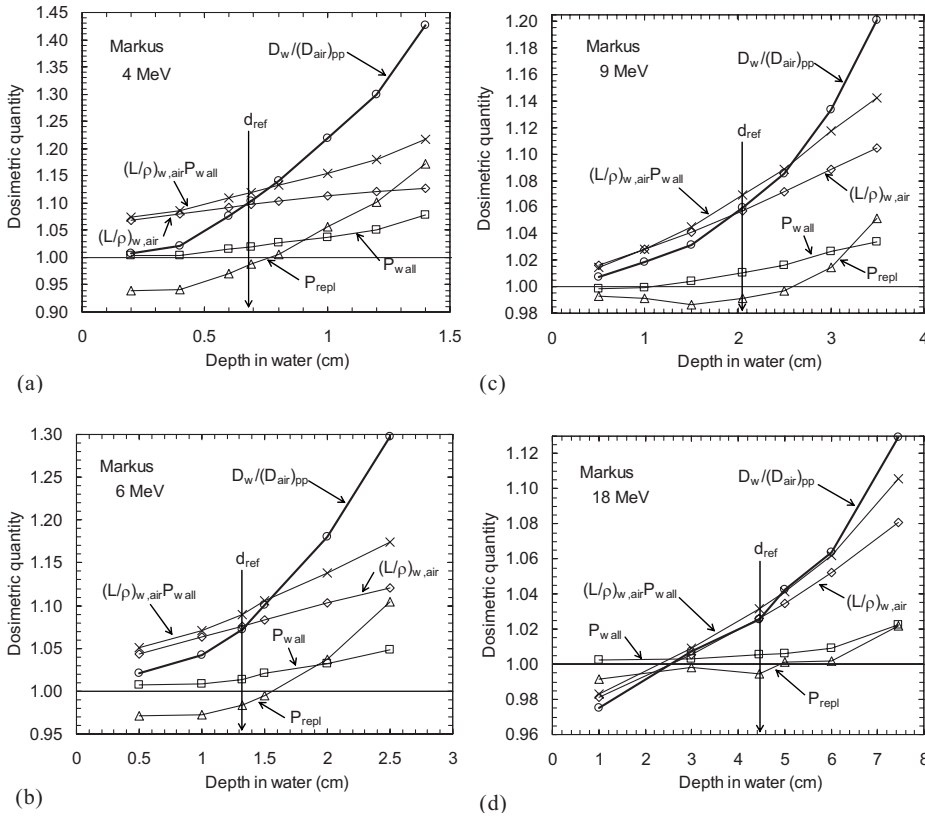


FIG. 4. Calculated dosimetric quantities for a Markus chamber as a function of depth at (a) 4, (b) 6, (c) 9, and (d) 18 MeV beams. For the Markus chamber, the protocol assumes that the ratio of doses $D_w/[D_{air}]_{pp}$ is equal to the product $(\bar{L}/\rho)_{air}^w P_{repl}$, but the dose ratio also depends on the variation of P_{wall} values. The dose ratio at a reference depth d_{ref} agrees with the simple stopping-power ratio because P_{wall} offsets P_{repl} .

RZnrc code. $[D_{air}]_w$ is the dose to the sensitive region in the chamber computed from the P_{wall} correction described above. Since P_{wall} is equal to unity in Fig. 2, P_{repl} is given from Eq. (2) as follows:

$$P_{repl} = \frac{D_w/[D_{air}]_w}{(\bar{L}/\rho)_{air}^w}. \quad (3)$$

$(\bar{L}/\rho)_{air}^w$ was calculated using the SPRRZnrc code. In recent study, Wang and Rogers¹⁰ calculated P_{repl} directly with “high density air” (HDA) and “low density water” (LDW) methods against an indirect SPR method [Eq. (3)] used in this study. As the result, it is found that the SPR method is in good agreement with HDA (0.001 mm thickness) and LDW methods. The geometries and materials for plane-parallel chambers used in this study are presented in detail in Table IV of the TRS-398 protocol. For a Markus chamber, a 0.87 mm Polymethyl Methacrylate (PMMA) waterproofing cap was used for the dose calculation in water.

III.C. Comparison of dosimetric quantities

The ratio of doses, $D_w/[D_{air}]_{pp}$, for NACP-02, Markus and Roos chambers was compared with the water-to-air stopping-power ratio to evaluate the overall correction factor (the product of P_{wall} and P_{repl}) presented in Eq. (2). D_w and $[D_{air}]_{pp}$ are calculated in Sec. III B. Furthermore, the dose ratio at d_{ref} was compared with that assumed by the TG-51 and TRS-398 protocols.

IV. RESULTS AND DISCUSSION

IV.A. Calculated P_{wall} and P_{repl}

Figures 3–5 show several of the factors involved in the dosimetry formalism in TG-51. The dosimetric quantities are calculated as a function of depth within the water phantom for NACP-02, Markus and Roos chambers, at 4, 6, 9, and 18 MeV beams. The depths are varied from near-surface to R_{50} for each beam. P_{wall} increases rapidly as a function of depth at lower energies for all the chambers. P_{wall} for NACP-02 varies from 1.004 at a depth of 0.2 cm to 1.136 at 1.4 cm for 4 MeV, from 1.004 to 1.079 for Markus and from 1.001 to 1.079 for Roos. NACP-02 composited with graphite and rexolite as a body material shows larger P_{wall} values than Markus and Roos made with PMMA because of its larger atomic number. Recently, Chin *et al.*¹⁹ reported that the front window mass thickness of NACP-02 is 35% greater than that listed in the TRS-398 protocol. This may also increase P_{wall} . The variation of P_{wall} for the plane-parallel chambers reduces with increasing electron energy. For 18 MeV, P_{wall} of NACP-02 ranges from 1.007 at a depth of 1 cm to 1.023 at 7.45 cm, from 1.002 to 1.023 for Markus and from 1.004 to 1.023 for Roos. The statistical uncertainties of the results computed with CAVRZnrc are 0.3%–0.5%, 0.4%–0.6%, and 0.25%–0.4% for NACP-02, Markus and Roos chambers, respectively, which are estimated with quadratic summation of the standard deviation (1σ) in doses for two geometries shown in Fig. 1. The magnitude of the variation in P_{wall} with depth for NACP-02 agrees well with results of Buckley and

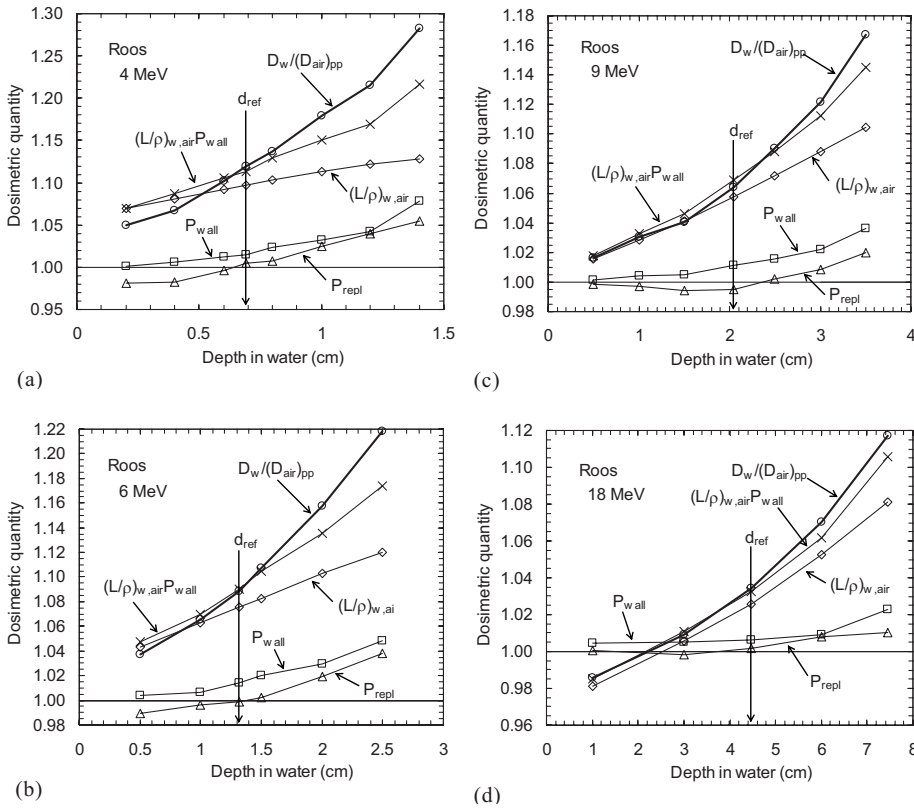


FIG. 5. Calculated dosimetric quantities for a Roos chamber as a function of depth at (a) 4, (b) 6, (c) 9, and (d) 18 MeV beams. For the Roos chamber, the protocol assumes that the ratio of doses $D_w/[D_{air}]_{pp}$ is equal to the water-to-air stopping-power ratio, but the dose ratio directly depends on the variation of P_{wall} and P_{repl} values. The dose ratio at a reference depth d_{ref} agrees with the product $(\bar{L}/\rho)_{air}^w P_{wall}$ because the P_{repl} value is close to unity.

Rogers.⁶ The P_{wall} values different from unity for the plane-parallel chambers is a drastic departure from standard dosimetry theory, especially for lower energy.

The variation of P_{repl} also increases rapidly as a function of depth at lower energies for all the chambers. P_{repl} for NACP-02 varies from 0.973 at a depth of 0.2 cm to 1.079 at 1.4 cm for 4 MeV, from 0.938 to 1.172 for Markus and from 0.982 to 1.055 for Roos. The variation of P_{repl} for Markus is huge compared to NACP-02 and Roos because of the narrow guard ring width. The variation of P_{repl} for the plane-parallel chambers also reduces as the electron energy increases. For 18 MeV, P_{repl} of NACP-02 ranges from 0.996 at a depth of 1 cm to 1.017 at 7.45 cm, from 0.992 to 1.022 for Markus and from 1.000 to 1.010 for Roos. The uncertainties of P_{repl} computed using the DOSRZnrc, CAVRZnrc, and SPRRZnrc codes are 0.3%–0.4%, 0.4%–0.5%, and 0.25%–0.35% for NACP-02, Markus and Roos chambers, respectively. The magnitude of the variation in P_{repl} with depth for NACP-02 agrees well with results of Wang and Rogers.¹⁰ The standard dosimetry protocols assume that P_{repl} is equal to unity for well-guarded plane-parallel chambers at all measurement depths. The P_{repl} values with depth increase drastically at the region with the steep dose gradient for lower energy. For Markus P_{repl} departs more than 10% from unity close to R_{50} . P_{repl} for NACP-02 and Roos chambers is close to unity in the plateau region of the depth-dose curves.

Figure 6 shows the calculated P_{wall} values at a reference depth as a function of R_{50} for each chamber and the values are in good agreement with the values reported in previous papers.^{6–8,15} The P_{wall} values decrease from 1.019 to 1.008 for NACP-02, from 1.019 to 1.005 for Markus, and from

1.015 to 1.006 for Roos, in a range of 4 MeV ($R_{50} = 1.31$ cm) to 18 MeV ($R_{50} = 7.6$ cm). The variation in P_{wall} with beam quality is approximately 1%.

Figure 7 shows the calculated P_{repl} values at a reference depth as a function of R_{50} for each chamber. P_{repl} for well-guarded chambers is close to unity at electron energies greater than or equal to 12 MeV ($R_{50} = 5.06$ cm) and consistent with that assumed by standard dosimetry protocols. The variations are larger for low energies, where they are $\pm 0.4\%$ and $\pm 0.5\%$ for the NACP-02 and Roos chambers, respectively. The results for each chamber are in good agreement with those of Wang and Rogers¹⁰ and Zink and Wulff,⁸ re-

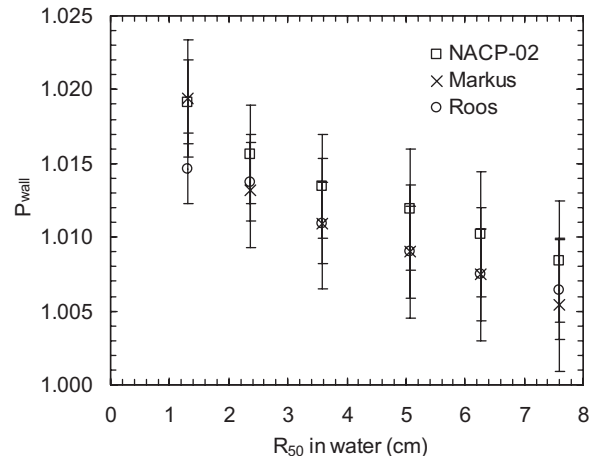


FIG. 6. Calculated P_{wall} at a reference depth as a function of R_{50} for NACP-02, Markus, and Roos chambers in a water phantom.

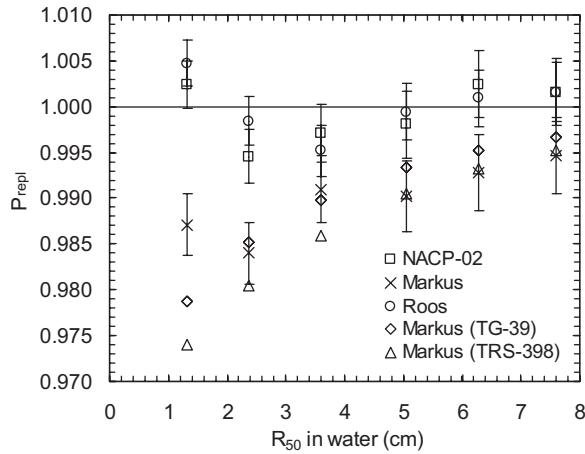


FIG. 7. Calculated P_{repl} at a reference depth as a function of R_{50} for NACP-02, Markus, and Roos chambers in a water phantom. Also shown are the P_{repl} values for Markus given by TG-39 (Ref. 18) and TRS-398 (Ref. 2).

spectively. For Markus, P_{repl} varies from 0.987 for 4 MeV to 0.995 for 18 MeV. The calculated P_{repl} values agree within 0.5% with the values recommended by TG-39 (Ref. 18) and TRS-398 that are based on experimental data,^{20,21} except for 4 MeV. The calculated result for 4 MeV is close to our measurement value of 0.983 (Ref. 22) but is approximately 1% larger than the protocols. The measurement for 4 MeV is difficult to perform precisely due to the steep dose gradient and the measurement thus involves a larger uncertainty. The P_{repl} value for TG-39 and TRS-398 is extrapolated from the regression formula.

IV.B. Comparison of dosimetric quantities

For the NACP-02 chamber, the standard dosimetry protocols assume that the ratio of doses, $D_w/[D_{\text{air}}]_{\text{pp}}$, is equal to the water-to-air stopping-power ratio, but the dose ratios directly depend on the variation in the P_{wall} and P_{repl} values with depth as shown in Fig. 3. In other words, the ratio of the dose ratio and stopping-power ratio curves corresponds to overall correction factor (the product of P_{wall} and P_{repl}). The dose ratio almost corresponds to the product $(\bar{L}/\rho)_{\text{air}}^w P_{\text{wall}}$ with increasing energy, except for a greater depth. The dose ratio at the reference depth also agrees with the product $(\bar{L}/\rho)_{\text{air}}^w P_{\text{wall}}$ at all beam energies.

For the Markus chamber in Fig. 4, the differences between the dose ratio and stopping-power ratio curves are much larger than those for the NACP-02 chamber because the magnitude of the variation in P_{repl} with depth is larger. The dose ratio at the reference depth shows better agreement with the stopping-power ratio because the effect of P_{wall} is cancelled by P_{repl} correction. The relationship of the dose ratio and the stopping-power ratio for the Roos chamber in Fig. 5 is similar to that for the NACP-02 chamber. The dose ratio at the reference depth is in better agreement with the product $(\bar{L}/\rho)_{\text{air}}^w P_{\text{wall}}$ than the stopping-power ratio at all beam energies.

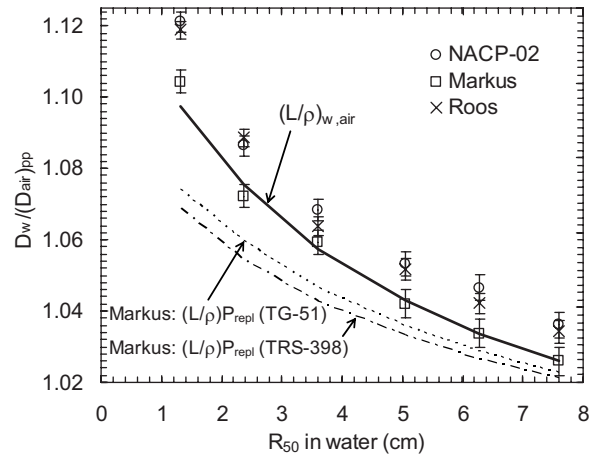


FIG. 8. The ratio of doses $D_w/[D_{\text{air}}]_{\text{pp}}$ at a reference depth for NACP-02, Markus, and Roos chambers as a function of electron beam quality. The dose ratio for NACP-02 and Roos chambers is shown in comparison to the water-to-air stopping-power ratio, which is that assumed by TG-51 and TRS-398. For Markus the dose ratio is compared with the product of the stopping-power ratio and P_{repl} recommended by TG-51 and TRS-398.

The overall correction factor affects significantly depth-dose measurements using the plane-parallel chambers at lower energies. The local dose at R_{50} increases by up to 18% at 4 MeV and 4% at 18 MeV for NACP-02. This is similar to results of Verhaegen *et al.*⁷ Similarly, the dose at R_{50} for Roos increases by up to 11% at 4 MeV and 3.5% at 18 MeV. For Markus the dose increases by up to 21% at 4 MeV and 5% at 18 MeV. However, the dose increment of 18% at R_{50} for 4 MeV increases the depth of R_{50} by only 0.5 mm for NACP-02. The effect becomes smaller with increasing the electron energy.

Figure 8 presents the dose ratio $D_w/[D_{\text{air}}]_{\text{pp}}$ at the reference depth for NACP-02, Markus and Roos chambers as a function of electron beam quality. The dose ratio for NACP-02 and Roos chambers is shown in comparison to the water-to-air stopping-power ratio, which is that assumed by TG-51 and TRS-398. The stopping-power ratios at d_{ref} of Burns *et al.*²³ adapted by TG-51 and TRS-398 agree within 0.2% with those calculated with the SPRZRnc code. For Markus the dose ratio is compared with the product of $(\bar{L}/\rho)_{\text{air}}^w$ and P_{repl} recommended by TG-51 and TRS-398. The dose ratio for NACP-02 and Roos chambers is about 1% larger than the water-to-air stopping-power ratio, in the range of 6–18 MeV and 2% larger at 4 MeV. The ratio of the dose ratio and the stopping-power ratio (the overall correction factor) for NACP-02 and Roos are 1.0100 and 1.0081, respectively, at $R_{50}=7.6$ cm. The factor for NACP-02 is in reasonable agreement with 1.0074 at $R_{50}=8.3$ cm estimated using the EGSnrc/CSnrc code by Buckley and Rogers.⁶ The results of Sempau *et al.*⁵ ($f_{c,Q}$ in their article) for NACP-02 and PPC-40 (Roos type) is approximately 0.5% higher than the stopping-power ratio of TRS-398 at $R_{50}=1.4$ cm. Their overall correction factor is assumed to be unity at $R_{50}=8.75$ cm. When the overall correction factor in this study is assumed to be unity at $R_{50}=7.6$ cm, the dose ratio for NACP-02 and Roos is approximately 1% higher than the stopping-power

ratio of TRS-398 at $R_{50}=1.31$ cm. This is in reasonable agreement with the result of Sempau *et al.*⁵ The overall collection factors for Roos also agree well with results of Zink and Wulff.⁸

The dose ratio for the Markus chamber increases from 0.5% to 3.3% and from 0.3% to 2.8%, respectively, compared to the values recommended by TG-51 and TG-398, in the range of 4 MeV ($R_{50}=1.31$ cm) to 18 MeV ($R_{50}=7.6$ cm). The dose ratio at the reference depth for Markus almost agrees with the stopping-power ratio of TG-51 and TRS-398 because the overall correction factor is almost equal to unity as seen in Fig. 4.

V. CONCLUSIONS

This article has investigated P_{wall} and P_{repl} correction factors for plane-parallel ionization chambers in clinical electron dosimetry using the EGSnrc Monte Carlo code system. The calculated P_{wall} values for NACP-02 increase from 1.005 to 1.136 for 4 MeV and from 1.007 to 1.023 for 18 MeV, at a depth between near-surface to R_{50} . Similarly, the P_{wall} values increase from 1.004 to 1.079 and from 1.002 to 1.023 for Markus (that is a classic design), and from 1.001 to 1.079 and from 1.004 to 1.023 for Roos. The P_{wall} values at a reference depth vary from 1.019 to 1.008 for NACP-02, from 1.019 to 1.005 for Markus, and from 1.015 to 1.006 for Roos, in a range of 4–18 MeV. The calculated P_{wall} values are different from the value of unity assumed by standard dosimetry protocols.

Also, the calculated P_{repl} values for NACP-02 increase from 0.973 to 1.079 for 4 MeV and from 0.996 to 1.017 for 18 MeV, at a depth between near-surface to R_{50} . Similarly, the P_{repl} values increase from 0.938 to 1.172 and from 0.992 to 1.022 for Markus, and from 0.982 to 1.055 and from 1.000 to 1.010 for Roos. The P_{repl} values at the reference depth for NACP-02 and Roos are close to unity in a range of 4–18 MeV. The P_{repl} values of Markus vary from 0.987 to 0.995 and agree with the values recommended by standard dosimetry protocols except for 4 MeV.

The overall correction factor affects significantly depth-dose measurements using the plane-parallel chambers at lower energies. Although the dose increment around R_{50} for 4 MeV is more than 10%, the effect increases the depth of R_{50} by only 0.5 mm for 4 MeV. The ratio of doses $D_w/[D_{\text{air}}]_{\text{pp}}$ at the reference depth for NACP-02 and Roos are about 1% larger than the water-to-air stopping-power ratio in the range of 6–18 MeV and 2% larger for 4 MeV. The dose ratio for Markus increases by up to approximately 3% compared to the product of the water-to-air stopping-power ratio and P_{repl} recommended by TG-51 and TRS-398 for 4 MeV. This study indicates the need for an overall correction factor for the use of plane-parallel chambers in standard dosimetry protocols.

ACKNOWLEDGMENTS

The author would like to thank Varian Oncology Systems for providing detailed treatment head designs to simulate Varian Clinac accelerators. This study was partially sup-

ported by a Grant in-Aid for Scientific Research (C), 19591460.

^{a)}Electronic mail: f_araki@kumamoto-u.ac.jp

¹P. R. Almond, P. J. Biggs, B. M. Coursey, W. F. Hanson, M. S. Huq, R. Nath, and D. W. O. Rogers, "AAPM's TG-51 protocol for clinical reference dosimetry of high-energy photon and electron beams," *Med. Phys.* **26**, 1847–1870 (1999).

²IAEA, "Absorbed dose determination in external beam radiotherapy: An international code of practice for dosimetry based on standards for absorbed dose to water," *Technical Report Series No. 398* (IAEA, Vienna, 2000).

³JSPM: Japanese Society of Medical Physics, "The standard dosimetry of absorbed dose in external beam radiotherapy," Tsusho-sangyo-kenkyusya, Tokyo, 2002 (in Japanese).

⁴IPEM, "The IPEM code of practice for electron dosimetry for radiotherapy beams of initial energy from 4 to 25 MeV based on an absorbed dose to water calibration," *Phys. Med. Biol.* **48**, 2929–2970 (2003).

⁵J. Sempau, P. Andreo, J. Aldana, J. Mazurier, and F. Salvat, "Electron beam quality correction factor for plane-parallel ionization chambers: Monte Carlo calculations using the PENELOPE system," *Phys. Med. Biol.* **49**, 4427–4444 (2004).

⁶L. A. Buckley and D. W. O. Rogers, "Wall correction factors, P_{wall} , for parallel-plate ionization chambers," *Med. Phys.* **33**, 1788–1796 (2006).

⁷F. Verhaegen, R. Zakikhani, A. DuSautoy, H. Palmans, G. Bostock, D. Shipley, and J. Seuntjens, "Perturbation correction factors for the NACP-02 plane-parallel ionization chamber in water in high-energy electron beams," *Phys. Med. Biol.* **51**, 1221–1235 (2006).

⁸K. Zink and J. Wulff, "Monte Carlo calculations of beam quality correction factors k_Q for electron dosimetry with a parallel-plate Roos chamber," *Phys. Med. Biol.* **53**, 1595–1607 (2008).

⁹M. McEwen, H. Palmans, and A. Williams, "An empirical method for the determination of wall perturbation factors for parallel-plate chambers in high-energy electron beams," *Phys. Med. Biol.* **51**, 5167–5181 (2006).

¹⁰L. L. W. Wang and D. W. O. Rogers, "Calculations of the replacement correction factors for ion chambers in megavoltage beams by Monte Carlo simulation," *Med. Phys.* **35**, 1747–1755 (2008).

¹¹I. Kawrakow and D. W. O. Rogers, "The EGSnrc code system: Monte Carlo Simulation of Electron and Photon Transport," National Research Council of Canada Report PIRS-701, 2002.

¹²D. W. O. Rogers, B. A. Faddegon, G. X. Ding, C. M. Ma, J. We, and T. R. Mackie, "BEAM: A Monte Carlo code to simulate radiotherapy treatment units," *Med. Phys.* **22**, 503–524 (1995).

¹³D. W. O. Rogers, C. Ma, G. X. Ding, B. R. Walters, D. Sheikh-Bagheri, and G. G. Zhang, "BEAMnrc user's manual," National Research Council of Canada Report PIRS-509 (a) Rev F, 2001.

¹⁴M. R. Bieda, J. A. Antolak, and K. R. Hogstrom, "The effect of scattering foil parameters on electron-beam Monte Carlo calculations," *Med. Phys.* **28**, 2527–2534 (2001).

¹⁵F. Araki, "Monte Carlo study of correction factors for the use of plastic phantoms in clinical electron dosimetry," *Med. Phys.* **34**, 4368–4377 (2007).

¹⁶C. M. Ma, D. W. O. Rogers, and B. R. Walters, "DOSXYZnrc user's manual," National Research Council of Canada Report PIRS-509 (b) Rev F, 2001.

¹⁷D. W. O. Rogers, I. Kawrakow, J. P. Seuntjens, B. R. Walters, and E. Mainegra-Hing, "NRC User Codes for EGSnrc," National Research Council of Canada Report PIRS-702 Rev B, 2005.

¹⁸P. R. Almond, F. H. Attix, L. J. Humphries, H. Kubo, R. Nath, S. Goetsch, and D. W. O. Rogers, "The calibration and use of plane-parallel ionization chambers for dosimetry of electron beams: An extension of the 1983 AAPM protocol report of AAPM Radiation Therapy Committee Task Group No. 39," *Med. Phys.* **21**, 1251–1260 (1994).

¹⁹E. Chin, D. Shipley, M. Bailey, J. Seuntjens, H. Palmans, A. DuSautoy, and F. Verhaegen, "Validation of a Monte Carlo model of a NACP-02 plan-parallel ionization chamber model using electron backscatter experiments," *Phys. Med. Biol.* **53**, N119–N126 (2008).

²⁰F. W. Wittkämper, H. Thierens, A. Van der Plaetsen, C. de Wagter, and B. J. Mijnheer, "Perturbation correction factors for some ionization chambers commonly applied in electron beams," *Phys. Med. Biol.* **36**, 1639–1652 (1991).

²¹A. Van der Plaetsen, J. Seuntjens, H. Thierens, and S. Vynckier, "Verifi-

cation of absorbed doses determined with thimble and parallel-plate ionization chambers in clinical electron beams using ferrous sulphate dosimetry," *Med. Phys.* **21**, 37–44 (1994).

²²F. Araki, Y. Shirakawa, R. Ikeda, T. Shimonobou, N. Moribe, T. Takada, M. Takahashi, H. Oura, and M. Matoba, "Determination of overall per-

turbation factors for plane-parallel ionization chambers in electron beams," *Jpn. Med. Phys.* **34**, 95–103 (2000).

²³D. T. Burns, G. X. Ding, and D. W. O. Rogers, " R_{50} as a beam quality specifier for selecting stopping-power ratios and reference depths for electron dosimetry," *Med. Phys.* **23**, 383–388 (1996).